

Linearized nonequilibrium dynamics in nonconformal plasma

ROMUALD A. JANIK^{*1}, GRZEGORZ PLEWA^{†2}, HESAM SOLTANPANAH^{‡1}, AND MICHAŁ SPALIŃSKI^{§2,3}

¹*Institute of Physics, Jagiellonian University, ul. Lojasiewicza 11, 30-348 Kraków, Poland*

²*National Center for Nuclear Research, ul. Hoża 69, 00-681 Warsaw, Poland*

³*Physics Department, University of Białystok, ul. Lipowa 41, 15-424 Białystok, Poland*

Abstract

We investigate the behaviour of the lowest nonhydrodynamic modes in a class of holographic models which exhibit an equation of state closely mimicking the one determined from lattice QCD. We compute the lowest quasinormal mode frequencies for a range of scalar self-interaction potentials and find that the damping of the quasinormal modes at the phase transition/crossover falls off by a factor of around two from conformality after factoring out standard conformal temperature dependence. The damping encoded in the imaginary part of the frequencies turns out to be correlated with the speed of sound and is basically independent of the UV details of the model. We also find that the dynamics of the nonhydrodynamic degrees of freedom remains ultralocal, even to a higher degree, as we deviate from conformality. These results indicate that the role of nonhydrodynamic degrees of freedom in the vicinity of the crossover transition may be enhanced.

*Email: romuald@th.if.uj.edu.pl

†Email: g.plewa@ncbj.gov.pl

‡Email: hesam@th.if.uj.edu.pl

§Email: mspal@fuw.edu.pl

Contents

1	Introduction	2
2	The nonconformal gravity backgrounds	4
3	Eddington-Finkelstein coordinates	6
4	Quasinormal modes	10
4.1	Introductory remarks	10
4.2	QNM of a massless scalar field	11
4.3	Numerical approach	12
5	Results	12
5.1	The imaginary part of the QNM frequencies — damping	13
5.2	The real part of the QNM frequencies	14
5.3	Ultralocality	15
5.4	Further examples	15
6	Conclusions	17

1 Introduction

The quark-gluon plasma produced in relativistic heavy-ion collisions at RHIC and LHC is very successfully described by phenomenological hydrodynamic models [1]. Nevertheless, it is quite clear that the hydrodynamic description is applicable only from a certain initial time after an inherently nonequilibrium initial phase of expansion. The estimation of this so-called ‘thermalization time’ has been at the focal point of much theoretical effort.

The main fundamental difficulty in studying such a problem from first principles is that when the plasma is strongly coupled we need a method which would be at the same time nonperturbative and which would work directly in Minkowski signature.

For these reasons, the methods of the AdS/CFT correspondence have been applied in this context although predominantly for the case of the conformal $\mathcal{N} = 4$ SYM theory [2, 3]. Despite that, the results obtained within this framework are very encouraging.

Firstly, the appearance of a hydrodynamical description of the resulting plasma system is not an input but rather a result from a much more general dual gravitational description which incorporates genuine nonhydrodynamical degrees of freedom. Thus one can study the transition to hydrodynamics and its properties. Secondly, it has turned out that at the transition to hydrodynamics, the components of the energy-momentum tensor in the local rest frame are still significantly anisotropic, meaning that the plasma is then still quite far from thermal equilibrium which indicates that the phrase ‘early thermalization’ used in this context is really a misnomer. Thirdly, for numerous initial conditions, the plasma behaves hydrodynamically with very good accuracy when the dimensionless product of the proper time and temperature $T\tau \sim 0.6 - 0.7$ [4, 5]. Before that nonequilibrium degrees of freedom¹ are typically very important.

It is worth mentioning also numerous important results on the dynamics of shock wave collisions [6, 7, 8] which we do not describe in more detail here.

Since the full nonlinear dynamics in the deeply nonequilibrium regime is very complicated as it is described by higher dimensional Einstein’s equations and can be studied essentially only using the methods of numerical general relativity, it was suggested in [9, 10] that it may be useful to incorporate just the lowest, least damped nonhydrodynamic degrees of freedom into the commonly used nonlinear hydrodynamic description. On the dual gravity side these degrees of freedom are the so-called quasinormal modes (QNM) of a finite temperature black hole. The 4D equations involving these nonequilibrium modes proposed in [11] take as an input from the gravitational description only their real and imaginary frequencies $\omega_{QNM} = \pm\omega_R + i\omega_I$. Moreover, it turns out that the dependence of these frequencies on the momentum k is very mild and can be neglected in a first approximation. This property leads to a certain ‘ultralocality’ of the dynamics of the nonequilibrium modes on top of a hydrodynamic flow.

All the above investigations were performed in the context of the conformal $\mathcal{N} = 4$ SYM theory which, by its very definition does not exhibit any kind of phase transition or crossover behaviour. It is thus very interesting to study what modifications to the above picture appear for a nonconformal theory. There are various ways to

¹In the present paper we use this term to denote all nonhydrodynamical degrees of freedom in the plasma.

model nonconformal theories within the AdS/CFT correspondence either following a top-down approach by studying a specific nonconformal theory with a known string theory construction, or a bottom-up approach where the gravitational background is phenomenologically fixed to give properties known from lattice QCD. In the present paper we decided to concentrate on the latter approach partly for simplicity and partly in order to deal with a gravitational system which has very similar equation of state to real QCD².

In this paper we will concentrate on the dynamics of the lowest nonhydrodynamic degrees of freedom in the nonconformal setting. In particular we will investigate how the damping of these modes changes when we approach the crossover temperature T_c (defined more precisely later). This answers an important question whether the role of nonhydrodynamic degrees of freedom becomes more important or less important closer to the phase transition. Secondly, we will investigate whether the ‘ultralocality’ property observed for $\mathcal{N} = 4$ SYM nonequilibrium degrees of freedom (QNM) still holds in the nonconformal case, especially close to the crossover/phase transition.

The plan of this paper is as follows. In section 2 we will review the family of gravitational backgrounds that we will consider. In sections 3 and 4 we will give some details on their explicit numerical construction and on our procedure for finding quasinormal mode frequencies. As far as we know such a procedure has not been employed so far in the literature and may be useful also in other contexts. There we will also discuss the relation of scalar QNM with the metric ones for these backgrounds and proceed, in section 5, to describe our results. We close the paper with conclusions.

2 The nonconformal gravity backgrounds

In this paper we will study a family of black hole backgrounds which follow from an action of gravity coupled to a single scalar field with a specific self interaction potential:

$$S = \int d^5x \sqrt{g} \left[R - \frac{1}{2} (\partial\phi)^2 + V(\phi) \right] \quad (1)$$

This family has been introduced by Gubser and collaborators in a series of papers [12, 13, 14] and used to mimic the QCD equation of state by a judicious choice of the potential. These backgrounds were then used to study bulk viscosity (which identically

²A paper investigating the complementary top-down approach appeared simultaneously [20].

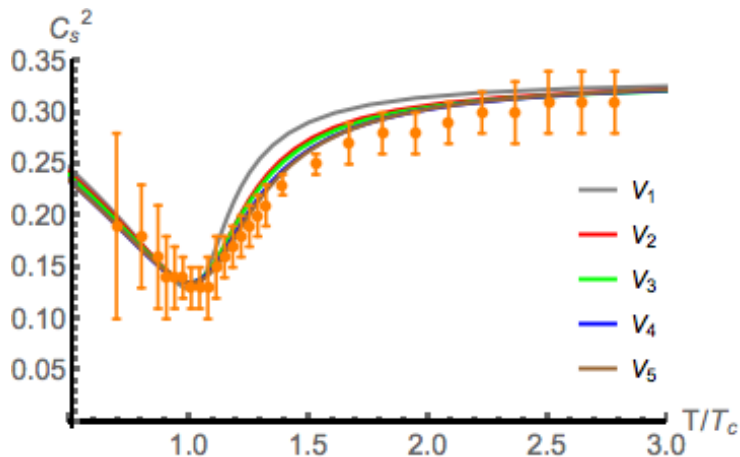


Figure 1: The speed of sound c_s^2 for the potentials $V_1 - V_5$ correspond to deformations of the theory by operators of dimensions 3.93, 3.67, 3.55, 3.10, 3.00 respectively given in table 1, together with Lattice QCD data from [16].

vanishes in the conformal case) and quite recently in [15], where second order hydrodynamic transport coefficients have been calculated. Ref. [12] provided an *approximate* but quite accurate formula for computing the equation of state (or more precisely the speed of sound c_s^2),

$$c_s^2 = \frac{d \log T}{d \log S} \quad (2)$$

directly in terms of the scalar potential $V(\phi)$. Thus the scalar potential parametrizes the physics of the particular type of gauge theory plasma.

The family of scalar potentials that we consider is

$$V(\phi) = -12 \cosh(b\phi) + c_2 \phi^2 + c_4 \phi^4 + c_6 \phi^6 \quad (3)$$

The quadratic terms in ϕ (mass term) determine, according to the standard AdS/CFT dictionary, the dimension Δ of the operator $\Delta(\Delta - 4) = m^2 L^2$, where L is the AdS radius which we fix it to one.

In this paper we will mostly concentrate on a set of parameter choices in (3) which approximately reproduce the equation of state of QCD plasma as determined by the Budapest-Wuppertal group in [16]. The resulting potentials are listed in table 1 and the corresponding speed of sound is shown in Fig. 1. In that figure we show the speed of sound extracted from a numerical construction of the corresponding black hole solution, as described in the following section, together with the lattice QCD data for c_s^2 . Note that in each case we are free to choose the units of temperature. Here,

potential	b	c_2	c_4	c_6	Δ
V_1	0.606	2.06	-0.1	0.0034	3.93
V_2	0.606	1.6	-0.1	0.0034	3.67
V_3	0.606	1.4	-0.1	0.0034	3.55
V_4	0.606	0.808	-0.1	0.0034	3.10
V_5	0.606	0.703	-0.1	0.0034	3.00

Table 1: The first group of potentials mimicking the QCD equation of state, together with the dimensions Δ of the relevant scalar operators. Potential V_6 in table 2 was first constructed in [12], while V_5 was recently used in [15].

following [15] we fix this freedom so that the temperature corresponding to the lowest dip in c_s^2 coincides for all the potentials. This will also be our provisional definition of the critical temperature T_c . According to [15] this value should be 143.8 MeV for QCD. Note finally that for high temperatures, the equation of state becomes essentially conformal. Similarly other properties such as the quasinormal frequencies also approach the conformal values characteristic of $\mathcal{N} = 4$ SYM at high temperature.

In order to check that the qualitative conclusions are generic, we also considered some other potentials leading to different profiles of $c_s^2(T)$. We will discuss them in section 5.4.

3 Eddington-Finkelstein coordinates

This section describes the black hole background solutions for the quasinormal mode calculations. These backgrounds are the same as those in [12], but since our goal is to determine the quasinormal mode frequencies, it will be convenient to express them in Eddington-Finkelstein coordinates, rather than in the coordinates used in [12]. We will discuss this in more detail in the following section on quasinormal modes.

The Ansatz for these solutions follows from the assumed symmetries: translation invariance in the Minkowski directions as well as $SO(3)$ rotation symmetry in the spatial part. This leads to the following form of the line element:

$$ds^2 = g_{tt}dt^2 + g_{xx}d\vec{x}^2 + g_{rr}dr^2 + 2g_{rt}drdt \quad (4)$$

where all the metric coefficients appearing in (4) are functions of the radial coordinate r alone, as is the scalar field ϕ . This form of the field Ansatz (determined so far only by the assumed symmetries) allows two gauge choices to be made. In [12] a Schwarzschild-

like gauge was adopted by taking $g_{tr} = 0$, accompanied by the condition $\phi = r$. The latter condition on the scalar field lead to key simplifications which were used to solve the field equations. The final form of the Ansatz in [12] was thus

$$ds^2 = e^{2A}(-h dt^2 + d\vec{x}^2) + \frac{e^{2B}}{h} dr^2 \quad (5)$$

$$\phi = r \quad (6)$$

where A , B , and h are functions of r (or, equivalently ϕ).

For the purpose of computing the quasinormal modes it is very convenient to use a different gauge – the Eddington-Finkelstein gauge $g_{rr} = 0$. It is typically convenient to also impose the gauge choice $g_{tr} = 1$, but for our purposes it turns out to be very effective to use the remaining gauge freedom to set $\phi = r$. Furthermore, if we label the metric components as

$$ds^2 = e^{2A}(-h dt^2 + d\vec{x}^2) - 2e^{A+B} dt dr \quad (7)$$

$$\phi = r \quad (8)$$

then the field equations take the form

$$A'' - A'B' + \frac{1}{6} = 0 \quad (9)$$

$$h'' + (4A' - B')h' = 0 \quad (10)$$

$$6A'h' + h(24A'^2 - 1) + 2e^{2B}V = 0 \quad (11)$$

$$4A' - B' + \frac{h'}{h} - \frac{e^{2B}}{h}V' = 0, \quad (12)$$

where the prime denotes a derivative with respect to ϕ .

With the assumed labelling of metric coefficients (5), equations (9)-(12) are identical to those of appearing in [12]. and so they can be solved following the method described there (see also [15]). In the remainder of this section we review this procedure for completeness.

We are interested in solutions possessing a horizon, which requires that the function h should have a zero at some $\phi = \phi_H$:

$$h(\phi_H) = 0, \quad (13)$$

It is easy to see that the solutions of Eq. (9)–(12) can be expressed in terms of a single

function $G(\phi) \equiv A'(\phi)$:

$$A(\phi) = A_H + \int_{\phi_H}^{\phi} d\tilde{\phi} G(\tilde{\phi}), \quad (14)$$

$$B(\phi) = B_H + \ln \left(\frac{G(\phi)}{G(\phi_H)} \right) + \int_{\phi_H}^{\phi} \frac{d\tilde{\phi}}{6G(\tilde{\phi})}, \quad (15)$$

$$h(\phi) = h_H + h_1 \int_{\phi_H}^{\phi} d\tilde{\phi} e^{-4A(\tilde{\phi})+B(\tilde{\phi})} \quad (16)$$

In the expressions above A_H , B_H , h_H and h_1 denote constants of integration which will be determined by requiring the appropriate near-boundary behaviour and eq. (13).

As in [12] by manipulating the field equations (9)-(12) one finds the nonlinear “master equation”

$$\frac{G'}{G + V/3V'} = \frac{d}{d\phi} \ln \left(\frac{G'}{G} + \frac{1}{6G} - 4G - \frac{G'}{G + V/3V'} \right) \quad (17)$$

The strategy is to solve this equation numerically by integrating it from the horizon at $\phi = \phi_H$ down toward the boundary at $\phi = 0$. Once G is known, the metric coefficients can be recovered from Eq. (14)-(16).

Solving Eq. (17) requires appropriate boundary conditions, which can be determined by evaluating (11) and (12) at the horizon and using (13). In this way one finds

$$V(\phi_H) = -3e^{-2B(\phi_H)}G(\phi_H)h'(\phi_H), \quad V'(\phi) = e^{-2B(\phi_H)}h'(\phi_H). \quad (18)$$

From this it follows that

$$G(\phi_H) = -\frac{V(\phi_H)}{3V'(\phi_H)}, \quad (19)$$

Using (19) and (17) one finds the following near-horizon expansion:

$$G(\phi) = -\frac{V(\phi_H)}{3V'(\phi_H)} + \frac{1}{6} \left(\frac{V(\phi_H)V''(\phi_H)}{V'(\phi_H)^2} - 1 \right) (\phi - \phi_H) + \mathcal{O}(\phi - \phi_H)^2 \quad (20)$$

In particular, the expansion (20) implies that

$$G'(\phi_H) = \frac{1}{6} \left(\frac{V(\phi_H)V''(\phi_H)}{V'(\phi_H)^2} - 1 \right). \quad (21)$$

To summarize: to find a numerical solution of (17) we can specify a value for ϕ_H and then use the conditions (19) and (21) as boundary conditions for integrating (17). There is however one technical complication in performing the numerical integration

outlined above: Eq. (19) implies that at the horizon

$$G(\phi_H) + V(\phi_H)/(3V'(\phi_H)) = 0 \quad (22)$$

which makes some terms of (17) singular. Even though such superficially singular terms cancel, their presence makes numerical computations troublesome. In order to circumvent this difficulty, instead of ϕ_H one can initialize the integration at a point just outside the horizon, at $\phi = \phi_H - \epsilon_H$, where $\epsilon_H \ll 1$. Then using (21) one can calculate $G(\phi_H - \epsilon_H)$ and $G'(\phi_H - \epsilon_H)$ and then use these values as the boundary conditions. One also needs to regularize at the boundary ($\phi = 0$) by integrating down to a small, but finite value $\phi = \epsilon_B$.

Having determined G , one can find the metric from (14)–(16). The constants of integration can be determined following [12]. The result is

$$\begin{aligned} A_H &= \frac{\ln \phi_H}{\Delta - 4} + \int_0^{\phi_H} d\phi \left[G(\phi) - \frac{1}{(\Delta - 4)\phi} \right] \\ B_H &= \ln \left(-\frac{4V(\phi_H)}{V(0)V'(\phi_H)L} \right) + \int_0^{\phi_H} \frac{d\phi}{6G(\phi)} \\ h_H &= 0 \\ h_1 &= \frac{1}{\int_{\phi_H}^0 d\phi e^{-4A(\phi)+B(\phi)}}. \end{aligned} \quad (23)$$

This way the metric is determined for any given choice of ϕ_H .

The Beckenstein-Hawking formula for entropy leads to the following expression for the entropy density

$$s = \frac{2\pi}{\kappa_5^2} e^{3A_H} \quad (24)$$

and the standard argument requiring non-singularity of the Euclidean continuation at the horizon gives

$$T = \frac{e^{A_H - B_H} |h'(r_H)|}{4\pi} \quad (25)$$

These equations lead to the formula

$$c_s^2 = \frac{d \log T / d\phi_H}{d \log s / d\phi_H} \approx \frac{1}{3} - \frac{1}{2} \frac{V'(\phi_H)^2}{V(\phi_H)^2}. \quad (26)$$

where the latter equality, proposed in [12], is only approximate but works surprisingly well. In the present paper when determining the speed of sound c_s^2 , we always use the exact formula and determine it from $d \log T / d \log s$ with temperature and entropy

extracted from the exact numerical solutions.

4 Quasinormal modes

4.1 Introductory remarks

It is convenient and enlightening to formulate the problem of finding quasinormal modes in terms of gauge invariant variables, which are diffeomorphism invariant linear combinations of the perturbations. This approach is well known in general relativity, and has been adopted in the holographic context in [10], where the conformal case of $\mathcal{N} = 4$ supersymmetric Yang-Mills theory was considered. The generalisation to the non-conformal cases was undertaken in [19]. In this section we briefly summarise our findings in the context of the models under consideration in this paper.

Under an infinitesimal diffeomorphism transformation, the metric and the scalar field fluctuations transform as the metric and the scalar field itself, i.e.

$$g_{\mu\nu} \rightarrow g_{\mu\nu} - \nabla_\mu \xi_\nu - \nabla_\nu \xi_\mu, \quad \phi \rightarrow \phi - \xi_\mu \nabla^\mu \phi. \quad (27)$$

By examining linear combinations of the linearized perturbations one finds five gauge invariant channels: two shear channels, one scalar channel, one sound channel and one bulk channel³ [19].

We assume the plane wave $e^{-i\omega t + i k x}$ dependence of the fluctuations on boundary coordinates t, x and some nontrivial dependence on the radial coordinate r . In general, the equations for the shear and scalar channels are decoupled from the rest, which have the same form as the conformal case. However the sound and bulk channels have coupled second order equations [19].

In the zero momentum limit, $k \rightarrow 0$, the equation for the sound mode becomes decoupled from the bulk mode and at the same time the equations for the other channels reduce to the equation for the QNM's of a massless scalar field, except for the equation of the bulk channel which is still coupled to the sound mode. Interestingly, this has two advantages. At $k = 0$ it is enough to find the QNM's for an external massless

³The bulk channel is a linear combination of transverse metric fluctuations and massive scalar fluctuation. One reason we call it "bulk" channel is it leads to non-zero bulk viscosity as well [13]. One could refer to it as the "non-conformal" channel and to the rest, which are already known in conformal case, as conformal channels.

scalar field for the conformal channels. On top of that, the coupling of the bulk mode with the sound mode means that the former has the same frequency as the latter. So in this limit, all the information about the QNM's of the theory is summarized in the QNM's of an external massless scalar field.

In view of this, the following analysis is focused on the QNM's of an external massless scalar field in the nonconformal backgrounds under consideration. Of course, in general it would still be interesting to study the metric and massive scalar field perturbations in detail.

4.2 QNM of a massless scalar field

In view of the results described in the previous section, we turn to exploring the effects of conformal symmetry breaking by considering the QNM of a massless scalar field Ψ in the background (7). As discussed earlier, the equation obtained for this case contains all the essential elements for QNM perturbations of the background.

The field equation for a massless scalar is simply the wave equation

$$\nabla_A \nabla^A \Psi = 0 \tag{28}$$

Quasinormal modes are solutions of the form

$$\Psi = e^{-i\omega t + ikx} \psi(\phi) \tag{29}$$

which satisfy the ingoing condition at the horizon, which in the Eddington-Finkelstein coordinate system reduces to regularity there. Substituting (29) into Eq. (28) and using the form of the background metric given in Eq. (7) leads to the following equation for the amplitude $\psi(\phi)$:

$$(3G V' + V)\psi'' - 3e^{-A-B}G'(e^{A+B}V' + 2i\omega)\psi' + 3e^{-2A-B}G'(k^2e^B - 3i\omega e^A G)\psi = 0. \tag{30}$$

where primes denote derivatives with respect to ϕ . Note that only the functions A and B appear here – the function h drops out. Since we are imposing two boundary conditions, this is an eigenvalue problem which can be solved only for specific values of the complex QNM frequency ω .

4.3 Numerical approach

Quite generally, the chief advantage of using the Eddington-Finkelstein coordinate system for finding quasinormal mode frequencies is twofold. Firstly, the ingoing boundary condition at the horizon gets translated just to ordinary regularity of the solution at the horizon. Secondly, due to the special form of the temporal part of Eddington-Finkelstein metric, the dependence on the mode frequency of the relevant differential equation is *linear*. Hence the problem of finding the quasinormal frequencies amounts to solving a linear ODE of the form

$$\hat{L}_1\Psi = \omega\hat{L}_2\Psi \tag{31}$$

where \hat{L}_1 and \hat{L}_2 are specific differential operators, with Ψ satisfying essentially Dirichlet boundary conditions at the boundary and being regular at the horizon. While many approaches to the problem of finding quasinormal modes have been described in the literature [17], we believe that the approach we describe here is very effective in conjunction with the spectral representation in terms of Chebyshev polynomials [18]. This representation reduces the task of solving Eq. (31) to a set of linear equations. The differential operators appearing in (31) are represented as matrices, and due to the linear dependence of this equation on ω this reduces to a generalized matrix eigenvalue problem which can be solved very efficiently.

In the case we are studying, the relevant equation is Eq. (30). This equation is indeed linear in ω . We have implemented the strategy outlined in the previous paragraph and verified the stability of the resulting solutions when varying the number of grid points in the Chebyshev discretization. The results of these numerical calculations are presented in section 5.

5 Results

We are interested in the dependence of the QNM frequencies on temperature and k in the vicinity of $k = 0$. Therefore, in line with the discussion in section 4.1, we focus on the quasinormal modes of an external massless scalar field. By use of the term “external” we wish to emphasize that this scalar is *distinct* from the scalar ϕ appearing in the background geometry, as QNM modes of the latter are mixed with

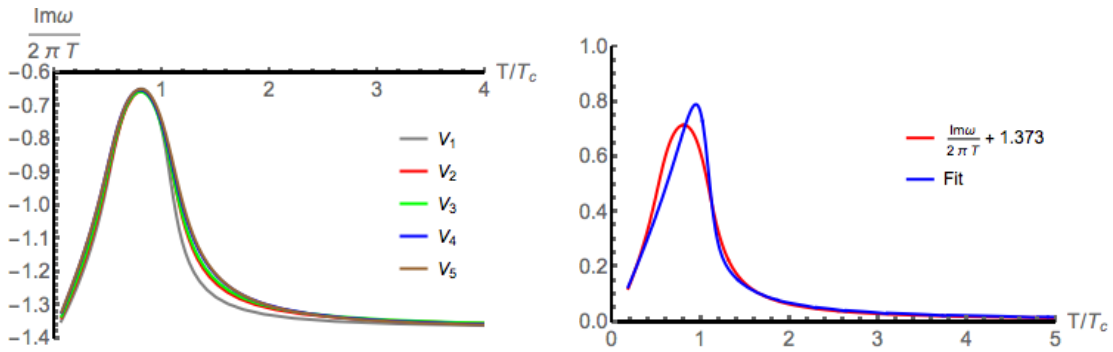


Figure 2: The imaginary parts of the lowest quasinormal mode at $k = 0$ for the potentials from table 1 (left). The imaginary part for potential V_2 together with the “phenomenological” according to Eq. (33) (right).

the metric perturbations⁴.

5.1 The imaginary part of the QNM frequencies — damping

In the left panel of figure 2 we show the imaginary parts of the QNM frequencies in units of temperature which is the natural scale in the problem i.e.

$$\frac{\text{Im } \omega}{2\pi T} \quad (32)$$

We observe that the damping significantly decreases (by a factor of 2) close to the transition. This shows that in the nonconformal case nonequilibrium dynamics become more important close to T_c . Moreover we find that the plots basically lie on top of each other for the various potentials from table 1. This indicates that the QNM frequencies are not sensitive to the fine details of the potentials but are essentially dependent just on the equation of state (speed of sound $c_s^2(T)$), which was the common denominator of all the potentials from table 1.

In order to parameterize the dependence of the damping on deviation from conformality, we propose a phenomenological formula expressing this as a linear combination of $c_s^2 - \frac{1}{3}$ and $T \frac{d}{dT} c_s^2(T)$. Specifically, we posit

$$\frac{\text{Im } \omega - \text{Im } \omega_{\text{conf}}}{2\pi T} = \gamma \left(c_s^2(T) - \frac{1}{3} \right) + \gamma' T \frac{d}{dT} c_s^2(T) \quad (33)$$

where γ, γ' are phenomenological parameters and $\frac{\text{Im } \omega_{\text{conf}}}{2\pi T} = -1.373$ is the conformal

⁴See the discussion in section 4.1

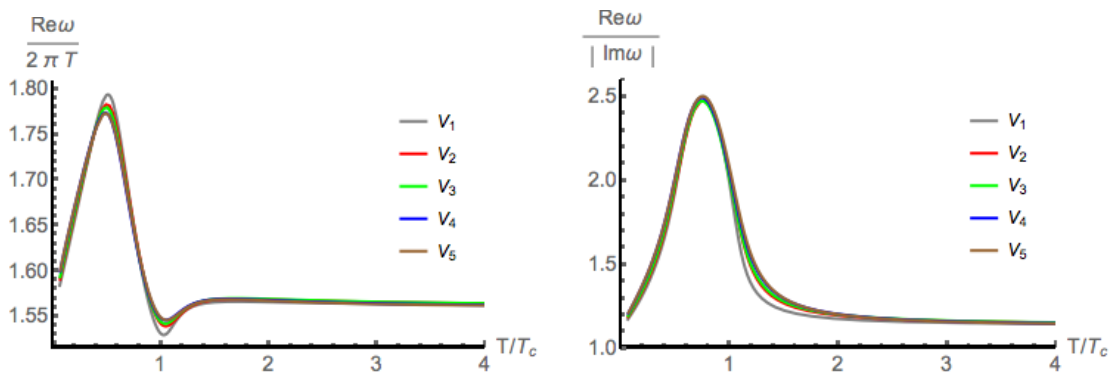


Figure 3: The real part of the lowest quasinormal mode at $k = 0$ for the potentials from table 1 (left) and the ratio of the real to the imaginary part (right).

limit value. These parameters can be fitted to the numerically calculated difference of the damping w.r.t the conformal case. For the potential V_2 in table 1 we got

$$\gamma = -3.729, \quad \gamma' = 0.452 \quad (34)$$

In figure 2(right) we show a plot of $(\text{Im}\omega - \text{Im}\omega_{\text{conf}})/(2\pi T)$ together with the fit. This two parameter fit is surprisingly good and may be thus used phenomenologically to estimate the damping in a nonconformal theory with the QCD equation of state. Since the quasinormal frequencies for the family of potentials we used in the left panel of figure 2 basically coincide, the single choice of parameters given in Eq. (34) works well for all of them.

5.2 The real part of the QNM frequencies

It is worth noting that similarly as for the imaginary part of the quasinormal frequencies, the real parts of the frequencies corresponding to the various potentials from table 1 are also very close to each other (see figure 3(left)). This signifies that the QNM frequencies are basically insensitive to differences in the UV (since the various potentials correspond to different Δ 's) and are governed by IR physics i.e. essentially the equation of state.

In figure 3(right), we also see an enhancement of the real part of the frequencies slightly below T_c .

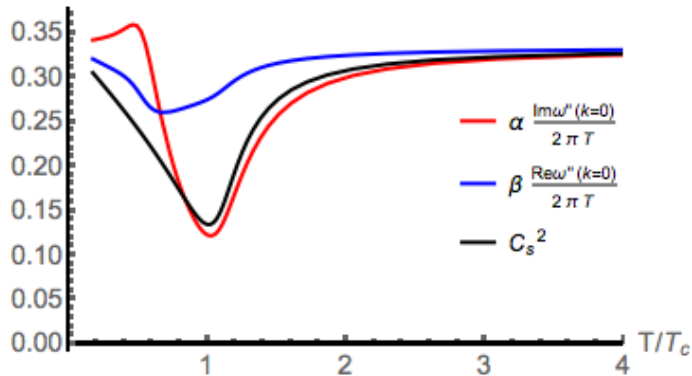


Figure 4: The curvature at $k = 0$ of the damping frequency, overlaid with $\alpha \simeq 1.114$ and $\beta \simeq 0.342$ for the potential V_2 in table 1.

5.3 Ultralocality

As indicated in the introduction, an interesting property of the dispersion relation for the nonhydrodynamic degrees of freedom in the conformal case of $\mathcal{N} = 4$ SYM theory is the very mild dependence of the frequencies ω_I and ω_R on the momentum k . In this section we show that for nonconformal theories this property holds to an even higher degree. Interestingly, the curvature of the damping i.e.

$$\frac{\text{Im } \omega''(k=0)}{2\pi T} \quad (35)$$

follows to a surprising accuracy (at least until $T \sim T_c$, then it starts to deviate) just the speed of sound c_s^2 , up to an overall numerical factor determined in the conformal high temperature limit (i.e. equivalently in $\mathcal{N} = 4$ SYM). The relevant plot is shown in figure 4. The plot for the other potentials in the same family are basically the same.

5.4 Further examples

As discussed in section 2, the choice of scalar potential translates into a specific equation of state for the QCD-like gauge theory. In this subsection we argue how the results discussed above apply to some additional cases listed in table 2.

The potentials V_6 and V_{11} have been introduced in [12]. The former was used to mimic the QCD equation of state using holography while the latter have a second-order phase transition at $T = T_c$. Fixing $b = 0.606$ corresponds to $c_s^2 = 0.15$ in the infrared [12]. The variety of potentials leads to a range of conformal weights $3 \leq \Delta \leq 3.93$ (table 2).

potential	b	c_2	c_4	c_6	Δ
V_6	0.606	2.06	0	0	3.93
V_7	0.606	1.8	0	0	3.79
V_8	0.606	1.145	0	0	3.37
V_9	0.606	0.808	0	0	3.10
V_{10}	0.606	0.703	0	0	3.00
V_{11}	$1/\sqrt{2}$	1.942	0	0	3.37

Table 2: The second group of potentials considered in the present paper.

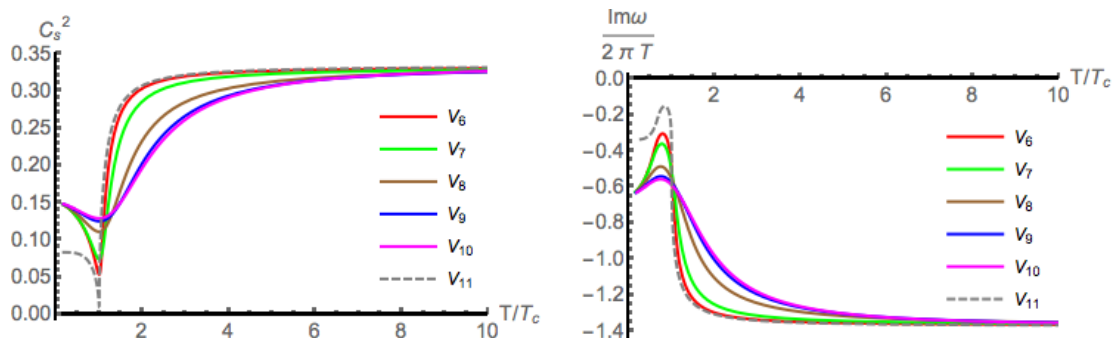


Figure 5: The speed of sound c_s^2 (left) and the imaginary parts of the lowest quasinormal modes at $k = 0$ (right) for the potentials from table 2. The one with cusp in the c_s^2 (left) corresponds to the most decreased in damping (right).

For all these cases the qualitative conclusions discussed earlier in this section still hold. In figure 5 we plot the speed of sound (left) and the imaginary parts of the lowest damped QNM's (right) for the potentials $V_6 - V_{11}$. Note that in all cases there is a critical temperature, corresponds to the lowest value of c_s^2 , which might be considered as the cross over/phase transition point (related to the potentials). Damping of the lowest QNM's decreases close to the $T = T_c$ by a factor of 2 – 7 (depending on the potential) relative to the conformal theory at high temperatures, figure 5 (right).

Figure 6 shows the momentum dependence of the imaginary part of QNM's (left) and the ratio of the real parts to the imaginary parts (right). The former indicates that ultralocality still holds for this more diverse class of potentials. Interestingly, comparing the plots in figure 5 (left) and 6 (left) suggest that the phenomenological relation we found in previous section,⁵ namely

$$c_s^2 \simeq 1.114 \frac{\text{Im } \omega''(k=0)}{2 \pi T} \quad (36)$$

is valid for this class of potentials too (again until $T \sim T_c$).

⁵The coefficient 1.114 is the same as "α" introduced in figure 4.

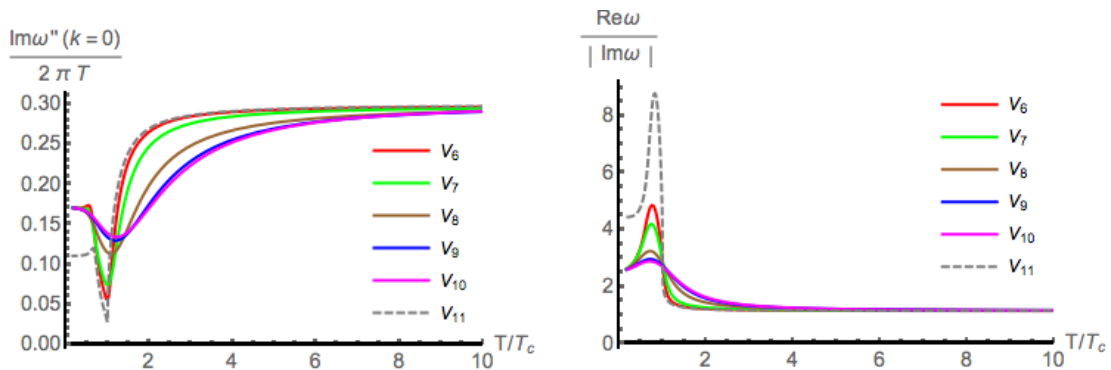


Figure 6: The curvature at $k = 0$ for the damping frequency for potentials from table 2 (left) and the ratio of the real to the imaginary part (right) for the same potentials.

The ratio of real parts to the imaginary parts of the lowest QNM's in figure 6 (right) shows a decreasing at $T \sim T_c$ i.e. the lower c_s^2 at $T = T_c$ the bigger decreasing in $\text{Re } \omega / \text{Im } \omega$.

Surprisingly, even the potential V_{11} with the second-order phase transition exhibits qualitatively the same behaviour as the other potentials discussed in the present paper.

6 Conclusions

In this paper we carried out a study of the lowest quasi-normal modes in a class of nonconformal holographic models which exhibit an equation of state very similar to the one obtained using lattice QCD. This class of models was introduced in [12] and incorporates 5-dimensional gravity coupled to a scalar field with a given self-interaction potential which parametrizes the model.

The frequencies of the lowest quasinormal modes provide a scale for the importance of nonhydrodynamic degrees of freedom, thus their determination is of a definite phenomenological interest. Our main observations are the following.

Firstly we found that, within the class of considered models, the imaginary part of the QNM frequency is strongly correlated with the speed of sound characteristic of the equation of state, once we factor out the trivial conformal temperature dependence. In particular, it decreases by a factor of around two at the point of the QCD crossover transition. This means that nonequilibrium effects will become more pronounced closer to the QCD phase transition/crossover. This seems to be a robust characteristic of this class of models and persists also for models with other equations of state considered

for completeness in section 5.4. We provided a phenomenological formula (33) linking the damping with the speed of sound. It is important to emphasize, that although the numerical values of the coefficients in (33) are specific *only* to the models mimicking the QCD equation of state, similar fits, with coefficients of the same sign and similar order of magnitude, work also for other models considered in section 5.4.

Secondly, we found that the quasinormal frequencies practically coincide for a whole class of models (potentials) which lead to the same equation of state (or more precisely to the same speed of sound $c_s^2(T)$ as a function of temperature). In particular, they seem to be quite independent of the particular UV properties of the concrete potential such as the anomalous dimension of the operator deforming the theory.

Thirdly, we found that the property of ultralocality found in [11], namely the very mild dependence of the quasinormal modes on the momentum k around $k = 0$ persists away from conformality. Even more so, it becomes more pronounced. We also noticed an intriguing feature that the curvature of the imaginary part of the QNM frequencies around $k = 0$ follows surprisingly well the speed of sound squared c_s^2 .

We believe that the above observations should be of phenomenological interest, especially as they indicate a more pronounced role of nonhydrodynamic degrees of freedom close to the QCD phase transition/crossover. It would be very interesting to gain some analytical understanding of these properties as well as to investigate directly nonlinear dynamical evolution in such models.

Acknowledgements. We thank Alex Buchel, Michał Heller and Rob Myers for sharing a draft of their preprint prior to submission. HS and MS would like to thank the organizers of the CERN-CKC TH Institute on Numerical Holography, where a part of this research was carried out. RJ and HS wish to thank Galileo Galilei Institute for Theoretical Physics for hospitality and the INFN for partial support during the program *Holographic Methods for Strongly Coupled Systems* where this work was finalized. RJ and HS were supported by NCN grant 2012/06/A/ST2/00396. GP and MS were supported by NCN grant 2012/07/B/ST2/03794.

References

- [1] E. Shuryak, “Heavy Ion Collisions: Achievements and Challenges,” arXiv:1412.8393 [hep-ph].
- [2] G. Policastro, D. T. Son and A. O. Starinets, “The Shear viscosity of strongly coupled $N=4$ supersymmetric Yang-Mills plasma,” Phys. Rev. Lett. **87** (2001) 081601 [hep-th/0104066].
- [3] P. Kovtun, D. T. Son and A. O. Starinets, “Viscosity in strongly interacting quantum field theories from black hole physics,” Phys. Rev. Lett. **94** (2005) 111601 [hep-th/0405231].
- [4] M. P. Heller, R. A. Janik and P. Witaszczyk, “The characteristics of thermalization of boost-invariant plasma from holography,” Phys. Rev. Lett. **108** (2012) 201602 [arXiv:1103.3452 [hep-th]].
- [5] J. Jankowski, G. Plewa and M. Spalinski, “Statistics of thermalization in Bjorken Flow,” JHEP **1412** (2014) 105 [arXiv:1411.1969 [hep-th]].
- [6] P. M. Chesler and L. G. Yaffe, “Holography and colliding gravitational shock waves in asymptotically AdS_5 spacetime,” Phys. Rev. Lett. **106** (2011) 021601 [arXiv:1011.3562 [hep-th]].
- [7] J. Casalderrey-Solana, M. P. Heller, D. Mateos and W. van der Schee, “From full stopping to transparency in a holographic model of heavy ion collisions,” Phys. Rev. Lett. **111** (2013) 181601 [arXiv:1305.4919 [hep-th]].
- [8] P. M. Chesler and L. G. Yaffe, “Holography and off-center collisions of localized shock waves,” arXiv:1501.04644 [hep-th].
- [9] D. T. Son and A. O. Starinets, “Minkowski space correlators in AdS / CFT correspondence: Recipe and applications,” JHEP **0209** (2002) 042 [hep-th/0205051].
- [10] P. K. Kovtun and A. O. Starinets, “Quasinormal modes and holography,” Phys. Rev. D **72** (2005) 086009 [hep-th/0506184].
- [11] M. P. Heller, R. A. Janik, M. Spaliński and P. Witaszczyk, “Coupling hydrodynamics to nonequilibrium degrees of freedom in strongly interacting quark-gluon plasma,” Phys. Rev. Lett. **113** (2014) 26, 261601 [arXiv:1409.5087 [hep-th]].

- [12] S. S. Gubser and A. Nellore, “Mimicking the QCD equation of state with a dual black hole,” *Phys. Rev. D* **78** (2008) 086007 [arXiv:0804.0434 [hep-th]].
- [13] S. S. Gubser, A. Nellore, S. S. Pufu and F. D. Rocha, “Thermodynamics and bulk viscosity of approximate black hole duals to finite temperature quantum chromodynamics,” *Phys. Rev. Lett.* **101** (2008) 131601 [arXiv:0804.1950 [hep-th]].
- [14] S. S. Gubser, S. S. Pufu and F. D. Rocha, “Bulk viscosity of strongly coupled plasmas with holographic duals,” *JHEP* **0808** (2008) 085 [arXiv:0806.0407 [hep-th]].
- [15] S. I. Finazzo, R. Rougemont, H. Marrochio and J. Noronha, “Hydrodynamic transport coefficients for the non-conformal quark-gluon plasma from holography,” *JHEP* **1502** (2015) 051 [arXiv:1412.2968 [hep-ph]].
- [16] S. Borsanyi, G. Endrodi, Z. Fodor, S. D. Katz, S. Krieg, C. Ratti and K. K. Szabo, “QCD equation of state at nonzero chemical potential: continuum results with physical quark masses at order mu^2 ,” *JHEP* **1208** (2012) 053 [arXiv:1204.6710 [hep-lat]].
- [17] E. Berti, V. Cardoso and A. O. Starinets, “Quasinormal modes of black holes and black branes,” *Class. Quant. Grav.* **26**, 163001 (2009) [arXiv:0905.2975 [gr-qc]].
- [18] P. Grandclement and J. Novak, “Spectral methods for numerical relativity,” *Living Rev. Rel.* **12**, 1 (2009) [arXiv:0706.2286 [gr-qc]].
- [19] P. Benincasa, A. Buchel and A. O. Starinets, “Sound waves in strongly coupled non-conformal gauge theory plasma,” *Nucl. Phys. B* **733** (2006) 160 [hep-th/0507026].
- [20] A. Buchel, M.P. Heller, R.C. Myers, “Equilibration rates in a strongly coupled nonconformal quark-gluon plasma”